Ganoderma lucidum spore oil induces apoptosis of breast cancer cells in vitro and in vivo by activating caspase-3 and caspase-9

Chunwei Jiao[a,b], Wang Chen[a], Xupeng Tan[a], Huijia Liang[a], Jieyi Li[a], Hao Yun[a], Chunyan He[a], Jiaming Chen[a], Xiaowei Ma[a], Yizhen Xie[a,b,*], Burton B. Yang[c,d,**]

[a] *Guangdong Yuewei Edible Fungi Technology Co., Ltd., Guangzhou, 510663, PR China*
[b] *State Key Laboratory of Applied Microbiology Southern China, Guangdong Provincial Key Laboratory of Microbial Culture Collection and Application, Guangdong Open Laboratory of Applied Microbiology, Guangdong Institute of Microbiology, Guangdong Academy of Sciences, Guangzhou, 510070, PR China*
[c] *Sunnybrook Research Institute, Toronto, M4N 3M5, Canada*
[d] *Department of Laboratory Medicine and Pathobiology, University of Toronto, Toronto, M5S 1A8, Canada*

ARTICLE INFO

ABSTRACT

Ethnopharmacological relevance: The mushroom *Ganoderma lucidum* (*G. lucidum*) is a traditional Chinese medicine reported to have a variety of pharmacological properties, including anti-cancer activity. *G. lucidum* spore oil (GLSO) is a lipid substance extracted from sporoderm-broken spore of *G. lucidum*. However, the effect of GLSO on breast cancer and the underlying molecular mechanism remain unclear.

Aim of the study: The aim of this study was to identify the effects of GLSO on breast cancer cells in vitro and in vivo as well as to investigate the mechanistic basis for the anticancer effect of GLSO.

Materials and methods: First, in vitro MDA-MB-231 cells were treated with GLSO (0.2, 0.4, and 0.6 μL/mL). The protein levels of B-cell lymphoma-2 (Bcl-2), Bcl-2-associated X (Bax), X-linked inhibitor of apoptosis (XIAP), total poly (ADP-ribose) polymerase (PARP), caspase-3 and caspase-8 were examined using western blotting. The mRNA expression levels of Fas-associated protein with death domain (FADD), TNF receptor-associated factor 2 (TRAF2), caspases-3, -8, -9 and Bax were examined using qRT-PCR. Second, in vivo the anticancer properties of GLSO were assessed by H&E, TUNEL and immunohistochemistry in BALB/c mice injected with 4T1 cells. In addition, the levels of caspase-9/caspase-3 signaling pathway proteins in tumor tissue were evaluated by immunoblotting. Finally, MDA-MB-231 cells were treated with caspase inhibitors to measure cell viability, the protein levels were examined with western blotting.

Results: The results in vitro showed that GLSO up-regulated the expression of Bax and caspase-3 in MDA-MB-231 cells, but had no effect on the expression of caspase-8. Moreover, the growth of tumors in vivo was significantly suppressed in the GLSO-treated group. The results of Western blot were consistent with in vitro. In vitro, co-treatment of MDA-MB-231 cells with caspase inhibitors reduced the inhibitory effect of GLSO on cell growth.

Conclusions: GLSO inhibits the growth of MDA-MB-231 cells and tumors in vivo by inducing apoptosis, which may be achieved through the mitochondrial apoptotic pathway.

1. Introduction

Breast cancer is one of the most common malignant tumor in women worldwide with a high morbidity and mortality. It is estimated that there are 2 million new cases and 630,000 deaths from breast cancer every year, accounting for 14% of all cancer-related deaths among women worldwide (Ferlay et al., 2019). The current standard treatments for breast cancer are surgery, radiotherapy, chemotherapy, and immunotherapy. However, these treatments can be associated with unnecessary side effects, leading to decreased quality of life. Therefore, there is an urgent need to develop safe and effective therapies for breast cancer.

The mushroom *Ganoderma lucidum* (*G. lucidum Leyss. ex Fr.*) *Karst*, also known as Reishi or Lingzhi, is a valuable traditional Chinese medicines (TCM) and has been recognized for its potent medicinal effects for more than 2000 years (Dan et al., 2016). In the past few

---

* Corresponding author. Guangdong Institute of Microbiology, Guangdong Academy of Sciences, Guangzhou, 510070, P. R. China.
** Corresponding author. Department of Laboratory Medicine and Pathobiology, University of Toronto, Toronto, M5S 1A8, Canada.
E-mail addresses: xyzgdim@sina.com (Y. Xie), byang@sri.utoronto.ca (B.B. Yang).

decades, many studies have showed the active components of *G. lucidum* and their biological effects as well as underlying mechanisms of action. It has been reported that *G. lucidum* possess anti-inflammatory (Akihisa et al., 2007; Ko et al., 2008), anti-tumor (Hu et al., 2002; Wu et al., 2012; Barbieri et al., 2017), hepatoprotective (Jang et al., 2014; Mowsumi et al., 2013), analgesic (Lam et al., 2008; Koyama et al., 1997), as well as anti-human immunodeficiency virus-1 (el-Mekkawy et al., 1998) activity. Since it has been proved to relieve fatigue and improve quality of life in breast cancer patients, *G. lucidum* is recommended as a traditional Chinese medicine adjuvant in cancer treatments, being widely used in complementary therapy (Zhao et al., 2012; Bao et al., 2012; Jin et al., 2016). To date, more than 300 active compounds have been isolated from *G. lucidum* fruiting bodies, mycelium and spores (Wu et al., 2013). They include amino acids, peptides, fatty acids, oligosaccharides, trace elements and polysaccharides, in particular, triterpenoids, of which more than 150 species have been isolated (Boh et al., 2007). The triterpenoids and polysaccharides are the major active components of *G. lucidum*, respectively, and have been studied extensively for their inhibitory effects on many cancers (Huie and Di, 2004). So far, most of the studies are concentrated on triterpenoid extracted from *G. lucidum* fruiting bodies or mycelia. There are only a few studies related to triterpenoids extracted from the sporoderm-broken spores. It has been reported that more triterpenoids are present in the spores compared with other parts of *G. lucidum* (Min et al., 1998). With the recent advances in sporoderm-breaking technology, increasing attention has turned to identify the chemical components of sporoderm-broken spores of *G. lucidum* (BSGL) and their versatile biological activities. A study found that BSGL contained abundant substances with greater bioactivity than the compounds in *G. lucidum* fruiting bodies (Guo et al., 2009). Another one showed that the polysaccharide content of broken *G. lucidum* spores was approximately 2 times higher than that of unbroken *G. lucidum* spores (Huang et al., 2006). Moreover, the growth of HepG2, a human liver cancer cell line, is significantly more inhibited by BSGL than that from unbroken spores (Zhao et al., 2006). However, little is known about the inhibitory effect of *G. lucidum* sporoderm-broken spore oil (GLSO) prepared by supercritical CO_2 extraction technology on breast cancer cell growth in vitro or in vivo.

Our previous study showed that GLSO can activate caspase-3 and caspase-9, two members of a family of proteases and that they are the primary mediators of apoptosis (Jiao et al., 2014). In general, caspases-2, -8, and -10 mediate apoptosis through the death receptor pathway, whereas caspases-3 and -9 act through the mitochondrial pathway. After activation of caspase-9, the process of intracellular death begins, and the downstream caspase-3 is activated. Total poly (ADP-ribose) polymerase (PARP) is used as a cleavage substrate which is cut by caspase-3. During this process, apoptotic signals are amplified, and death signals are transmitted. In addition, X-linked inhibitor of apoptosis protein (XIAP) is an inhibitor of apoptosis, which directly inhibits caspases and regulates apoptosis in multiple ways (Chawla-Sarkar et al., 2001).

In the present study, we examined the effects of GLSO on breast cancer cells and explored the underlying molecular mechanisms of its anti-cancer activity. It is found that GLSO effectively inhibited the proliferation of MDA-MB-231 cancer cells in vitro and the growth of 4T1 tumors in vivo by regulating key genes and proteins involved in apoptosis.

2. Materials and methods

2.1. Preparation and analysis of extracts

The *G. lucidum* fruiting bodies were grown in the Dabie Mountains (Anhui Province, China) in September 2017 which were planted by Guangdong Yuewei Edible Fungus Technology Co., Ltd. and *G. lucidum* spores were collected during the ripening period of *G. lucidum*.

Sporoderm-broken spores of *G. lucidum* were extracted by supercritical CO_2 carbon dioxide extraction to produce GLSO. The specific experimental methods have applied for Chinese patent (ZL200610035574.8).

Glyceryl trilinoleate (CAS: 537-40-6), 1,2-Dilinoleoyl-3-oleoyl-*rac*-glycerol (CAS: 2190-21-8), 1,2-Dilinoleoyl-3-palmitoyl-*rac*-glycerol (CAS: 2190-15-0), 1,2-dioleoyl-3-linoleoyl-*rac*-glycerol (CAS: 2190-20-7), 1-Palmitoyl-2-oleoyl-3-linoleoyl-*rac*-glycerol (CAS: 1587-93-5), glyceryl trioleate (CAS: 122-32-7), 1,2-Dioleoyl-3-palmitoyl-*rac*-glycerol (CAS: 2190-30-9), 1,2-Dioleoyl-3-stearoyl-*rac*-glycerol (CAS: 2410-28-8), were purchased from sigma. Each sample was accurately weighed 25mg and dissolved in pure ethanol to 50 mL volumetric flask to prepare a mixed standard solution.

GLSO was accurately weighed 0.3g and dissolved in pure ethanol to 50 mL volumetric flask. HPLC analyses of the samples were carried out on Diamonsil C18 (5 µm, 250 × 4.6 mm) column and Waters SymmetryShield RP18 (5 µm, 250 × 4.6 mm) column in series. The mobile phase consisted of 40% isopropanol and 60% acetonitrile in a gradient elution program, The column temperature was set at 35 °C. The flow rate was set at 1 mL/min. The injection volume was 10 µL. The Evaporative light Scattering Detector (ELSD) program was as follows: photomultiplier light gain 5, drift tube temperature 40 °C, ELSD chamber temperature 50 °C, nebuliser pressure 25 psi.

2.2. Cell culture

Human breast carcinoma cell line MDA-MB-231 and mouse breast carcinoma cell line 4T1 were purchased from the China Center for Type Culture Collection. Cells were cultured in DMEM (gibco, C11095500BT) supplemented with 10% fetal bovine (gibco, 10099-141) serum at 37 °C in a humidified 5% CO_2 atmosphere.

2.3. Cell viability assay

Cell viability was assessed by Trypan blue staining. The cell suspension was mixed with an equal volume of 0.4% Trypan blue (Solarbio, C0040) and incubated for 2 min. After mixing, the cells were plated and counted using an automated cell counter.

2.4. Mouse tumor model

All experimental procedures were conducted according to the Guide for the Use and Care of Laboratory Animals of the National Institutes of Health and were in compliance with Animal Welfare Act Regulations. The study was approved by the Committee of the Guangdong Institute of Microbiology Animal Center (Permit Number: SYXK(YUE) 2016-0156). Four-week-old female BALB/c mice were maintained in a specific pathogen-free environment. After 2 weeks of adaptation, the mice were injected subcutaneously in the left armpit with 4T1 cells (8×10^4 cells/100 µl DMEM) and then randomized into treatment groups as follows: model group (saline, n = 12), GLSO group (6 g/kg, n = 12), both of which were administered once daily by oral gavage, and paclitaxel (PTX) group (n = 12), which received 10 mg/kg PTX twice weekly by intraperitoneal injection. Body weights were measured every three days. Tumor growth was monitored daily and used a digital Vernier caliper to measure the length and width when it was palpable (0.01 mm accuracy). Tumor volume (mm^3) was calculated as: V = (length × $width^2$)/2 (Naito et al., 1986). After 3 weeks of treatment, the mice were sacrificed, and the tumors were excised and weighed. One half of the tumor was fixed in 10% neutral formalin and processed for hematoxylin and eosin (H&E) staining, and the other half was snap-frozen in liquid nitrogen and stored at −80 °C for subsequent analysis.

2.5. RNA exaction and quantitative real-time PCR

Total RNA was extracted from MDA-MB-231 cells using an RNA extraction kit (Aidlab Biotech) according to the manufacturer's

Table 1
Primer sequences used for qRT-PCR.

Primer name		Sequences number (5' to 3')
FADD	forward	ACGCTTCGGAGGTAGATG
	reverse	CCTGGTACAAGAGGTTCA
TRAF2	forward	CACCGGTACTGCTCCTTCTG
	reverse	TGAACACAGGCAGCACAGTT
Caspase-8	forward	TGGTTCATCCAGTCGCTTTG
	reverse	AATTCTGTTGCCACCTTTCG
Caspase-9	forward	CTGTCTACGGCACAGATGGAT
	reverse	GGGACTCGTCTTCAGGGGAA
Caspase-3	forward	TGGTGATGAAGGGGTCATTTATG
	reverse	TTCGGCTTTCCAGTCAGACTC
Bax	forward	TGAAGACAGGGGCCTTTTTG
	reverse	AATTCGCCGGAGACACTCG
β-actin	forward	CTGGAACGGTGAAGGTGACA
	reverse	AAGGAACTTCCTTGAACAATGCA

Table 2
Key reagents table.

Reagents	Source	Identifier
glyceryl trilinoleate	Sigma	CAS:537-40-6
1,2-Dilinoleoyl-3-oleoyl-*rac*-glycerol	Sigma	CAS:2190-21-8
1,2-Dilinoleoyl-3-palmitoyl-*rac*-glycerol	Sigma	CAS:2190-15-0
1,2-Dioleoyl-3-linoleoyl-*rac*-glycerol	Sigma	CAS:2190-20-7
1-Palmitoyl-2-oleoyl-3-linoleoyl-*rac*-glycerol	Sigma	CAS:1587-93-5
glyceryl trioleate	Sigma	CAS:122-32-7
1,2-Dioleoyl-3-palmitoyl-*rac*-glycerol	Sigma	CAS:2190-30-9
1,2-Dioleoyl-3-stearoyl-*rac*-glycerol	Sigma	CAS:2410-28-8
RIPA buffer	Sigma	R0278
Anti-PARP antibody	Abcam	ab74290
Anti-XIAP antibody	Abcam	ab21278
Anti-Caspase-9 antibody	Abcam	ab202068
Anti-Caspase-8 antibody	Abcam	ab25901
Anti-Caspase-3 antibody	Abcam	ab13847
Anti-alpha Tubulin antibody	Abcam	ab52866
Anti-Cytochrome C antibody	Abcam	ab133504
Anti-rabbit IgG antibody	Abcam	ab6721
Anti-Bax antibody	Abcam	ab32503
Anti-Bcl-2 antibody	Abcam	ab32124
AZ10417808	ApexBio	A4416
Z-IETD-FMK	ApexBio	B3232
Z-LEHD-FMK	ApexBio	B3233
3,3-diaminobenzidine	Solarbio	DA1010
4',6-diamidino-2-phenylindole(DAPI)	Servicebio	G1012
Triton X-100	Servicebio	G1204
TUNEL reagent	Roche	11684817910
DMEM	Gibco	C11095500BT
Fetal bovine serum	Gibco	10099–141
Trypan blue	Solarbio	C0040

instructions. The quantity and quality of RNA were analyzed by NanoDrop One Microvolume UV–Vis Spectrophotometer (Thermo Fisher Scientific). Total RNA (1 μg/sample) was reverse transcribed with an iScript cDNA synthesis kit (TaKaRa). Real-time PCR was performed using SYBR PCR master mix (Applied Biosystems/Thermo Fisher Scientific) and a QuantStudio™ 6 Flex Real-time PCR system (Thermo Fisher Scientific). β-Actin was amplified as a reference gene. The PCR conditions were 40 cycles of 5 s denaturation at 95 °C, 30 s annealing at 55 °C, and 5 s extension at 65 °C. The relative expression of mRNA for each sample was calculated as follows: $\Delta Ct = Ct$ (sample) $-$ Ct (β-Actin), $\Delta\Delta Ct$ (sample) $= \Delta Ct$ (sample) $- \Delta Ct$ (calibrator). The fold change in mRNA was calculated through relative quantification ($2^{-\Delta\Delta Ct}$). Table 1 shows the primer sequences used for amplification of Fas-associated protein with death domain (FADD), TNF receptor-associated factor 2 (TRAF2), caspases-3, -8, -9, Bax and β-Actin (see Table 2).

2.6. Western blot analysis

After treatment, MDA-MB-231 cells and tumor tissues were lysed with ice-cold RIPA buffer (Sigma-Aldrich, R0278). The supernatants were collected after cell lysates were centrifuged at 12,000 rpm for 10 min at 4 °C, and used a BCA assay kit (Thermo Fisher Scientific) to measure the protein concentration. 10–15% SDS-PAGE to separate protein samples (40 μg/lane) and transferred to polyvinylidene fluoride membranes (Immobilon, USA). The membranes were blocked with 5% skim milk in Tris-buffered saline with 0.1% Tween-20 (TBST) for 2 h at room temperature, and then incubated overnight at 4 °C with primary antibodies (Abcam, Shanghai China) against B-cell lymphoma-2 (Bcl-2, ab32124), Bcl-2-associated X (Bax, ab32503), total poly (ADP-ribose) polymerase (PARP, ab74290), X-linked inhibitor of apoptosis (XIAP, ab21278), caspase-9 (ab202068), caspase-8 (ab25901), caspase-3 (ab13847), or tubulin (ab52866). The membranes were washed three times with TBST for 10 min each and then incubated with horseradish peroxidase-conjugated secondary antibody (Abcam, ab6721) for 1 h at room temperature. Protein signals were detected using ECL chemiluminescence reagent (Thermo Fisher Scientific).

2.7. H&E staining and TUNEL assay

Formalin-fixed paraffin-embedded tumor tissues were cut into 4-μm sections and stained with H&E for pathological evaluation. The TUNEL assay was performed using an In Situ Cell Death Detection Kit (Roche, 11684817910) according to the manufacturer's instructions. Briefly, tumor sections were deparaffinized, permeabilized with 0.2% Triton X-100 (Servicebio, G1204), and incubated with TUNEL reagent containing TMR red-labeled nucleotides at 37 °C for 1 h. The sections were then washed with PBS and mounted in medium containing 4',6-diamidino-2-phenylindole (DAPI, Servicebio, G1012). Fluorescence images were captured using a NIKON fluorescence microscope (NIKON ECLIPSE C1, Japan) at 40 × magnification.

2.8. Immunohistochemistry staining

For immunohistochemistry, additional sections were deparaffinized through a graded series of dimethylbenzene and ethanol, and antigens were retrieved by incubation in citric acid buffer (pH 6.0) at 100 °C for 20 min. The sections were incubated with 3% H_2O_2 for 25 min to block endogenous peroxidase activity and then with 1% goat serum albumin for 25 min to block nonspecific binding. The sections were incubated overnight at 4 °C with the following primary antibodies (all from Abcam) diluted in PBS: caspase-9 (ab202068, 1:300), Bax (ab32503, 1:500), X-linked inhibitor of apoptosis (XIAP, ab21278, 1:500) or cytochrome *c* (ab133504, 1:500). After washing, the sections were incubated with goat anti-rabbit IgG antibody (ab6721, 1:500 in PBS) for 50 min at room temperature. The sections were then washed again, incubated with 3,3-diaminobenzidine (Solarbio, DA1010), washed and counterstained with hematoxylin. The sections were finally mounted and imaged using a microscope (Kantao Technology, China).

2.9. Statistical analysis

The SPSS 19.0 software (IBM, Armonk, NY, USA) was used for statistical analysis. The data are presented as mean ± S.D.. Comparisons among the different groups were performed by the one-way analysis of variance (ANOVA). A probability value of $P < 0.05$ was considered significant.

3. Results

3.1. Chemical analysis of GLSO

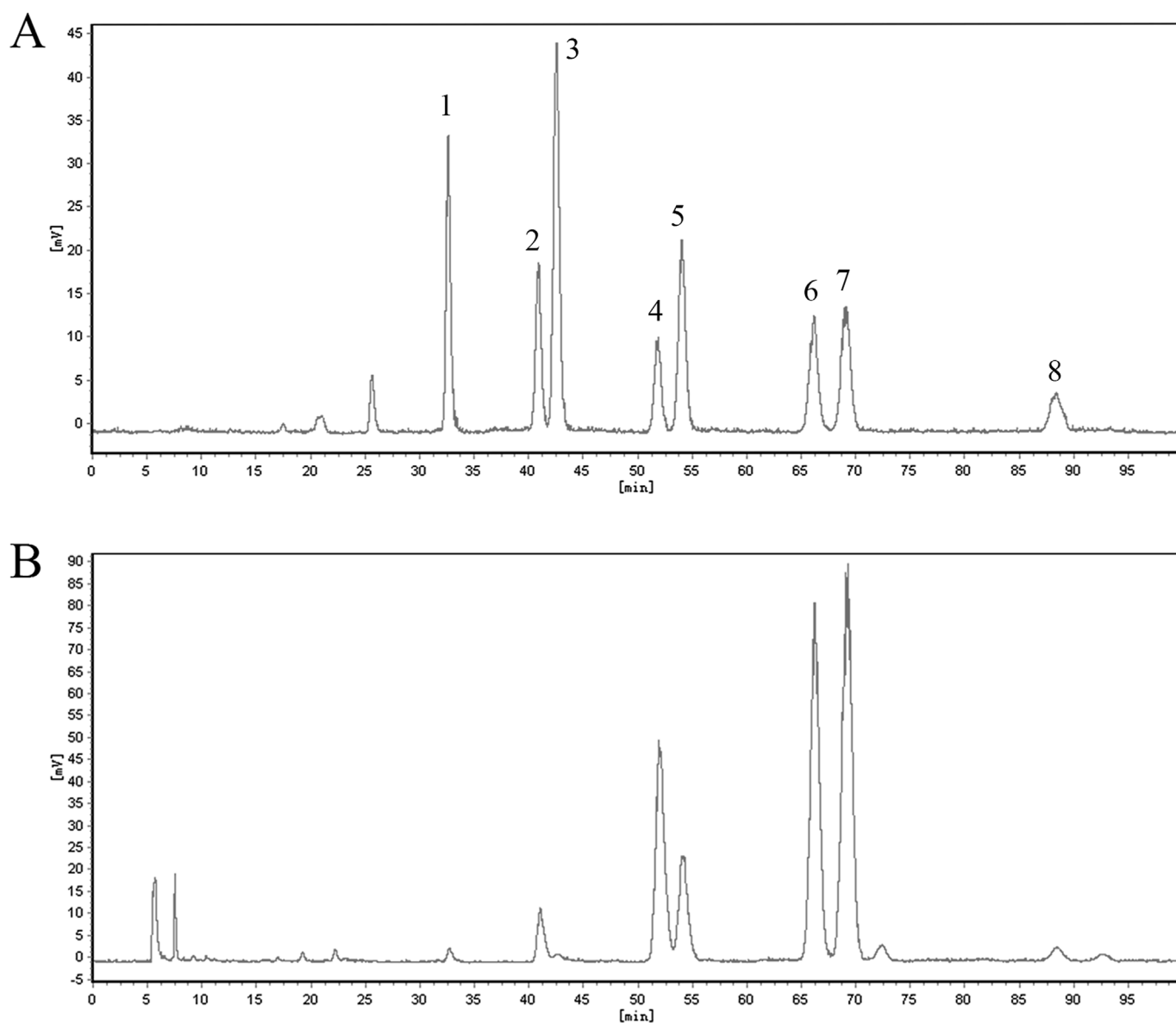Eight glyceride components in GLSO were determined by HPLC

Fig. 1. HPLC chromatograms. (A) Reference substance. (B) Sample of GLSO. (1) Glyceryl trilinoleate, (2) 1,2-Dilinoleoyl-3-oleoyl-*rac*-glycerol, (3) 1,2-Dilinoleoyl-3-palmitoyl-*rac*-glycerol, (4) 1,2-Dioleoyl-3-linoleoyl-*rac*-glycerol, (5) 1-Palmitoyl-2-oleoyl-3-linoleoyl-*rac*-glycerol, (6) Glyceryl trioleate, (7) 1,2-Dioleoyl-3-palmitoyl-*rac*-glycerol, (8) 1,2-Dioleoyl-3-stearoyl-*rac*-glycerol.

(Fig. 1). The results showed that the higher content of glyceride in GLSO was 1,2-Dioleoyl-3-palmitoyl-*rac*-glycerol, glyceryl trioleate, 1,2-dioleoyl-3-linoleoyl-rac-glycerol, 1-palmitoyl-2-oleoyl-3-linoleoyl-rac-glycerol and 1,2-dilinoleoyl-3-oleoyi-rac-glycerol, these components account for about 90% of the total. Among them, 1,2-Dioleoyl-3-palmitoyl-*rac*-glycerol and glyceryl trioleate account for 50% of the total.

3.2. GLSO inhibits proliferation and induces apoptosis of MDA-MB-231 breast cancer cells in vitro

Previous experiments have shown that GLSO had an inhibitory effect on breast cancer cells (Jiao et al., 2014). To determine the effect of GLSO on MDA-MB-231 breast cancer cells. Several key molecules involved in apoptosis were analyzed by RT-PCR and Western blot. As shown in Fig. 2A–E, GLSO induced significant downregulation of the anti-apoptotic molecules Bcl-2 and XIAP, and significant upregulation of the pro-apoptotic molecules FADD, caspase-3, caspase-9, and Bax, and had no effect on caspase-8. In addition, total level of PARP, a DNA repair enzyme, was also reduced in GLSO-treated MDA-MB-231 cells.

Collectively, these data suggest that GLSO induces apoptosis in MDA-MB-231 cells through a caspase-3 mediated pathway Fig. 1.

3.3. GLSO inhibits growth of mouse breast cancer tumors in vivo

To evaluate whether the pro-apoptotic effects of GLSO were also seen in vivo, BALB/c mice were injected with the mouse breast cancer cell line 4T1, and administered saline (model group) or GLSO (6 g/kg) once daily orally or PTX (10 mg/kg) twice weekly by intraperitoneal injection. After 3 weeks, the mice were sacrificed and the tumors were excised for analysis. As shown in Fig. 2, there was no significant difference in tumor volume between the GLSO-treated and PTX-treated group, but the tumor volume in GLSO-treated group was significantly smaller than the model group ($p < 0.01$, Fig. 3A). The tumors in the GLSO-treated group grew significantly more smaller and lighter than those in the model group after 21 days ($p < 0.05$, Fig. 3B, C). Notably, although GLSO-treated mice showed a modest decrease in body weight compared with the model and PTX groups in the final week, the change was not significant (Fig. 3D). Nevertheless, no other adverse effects
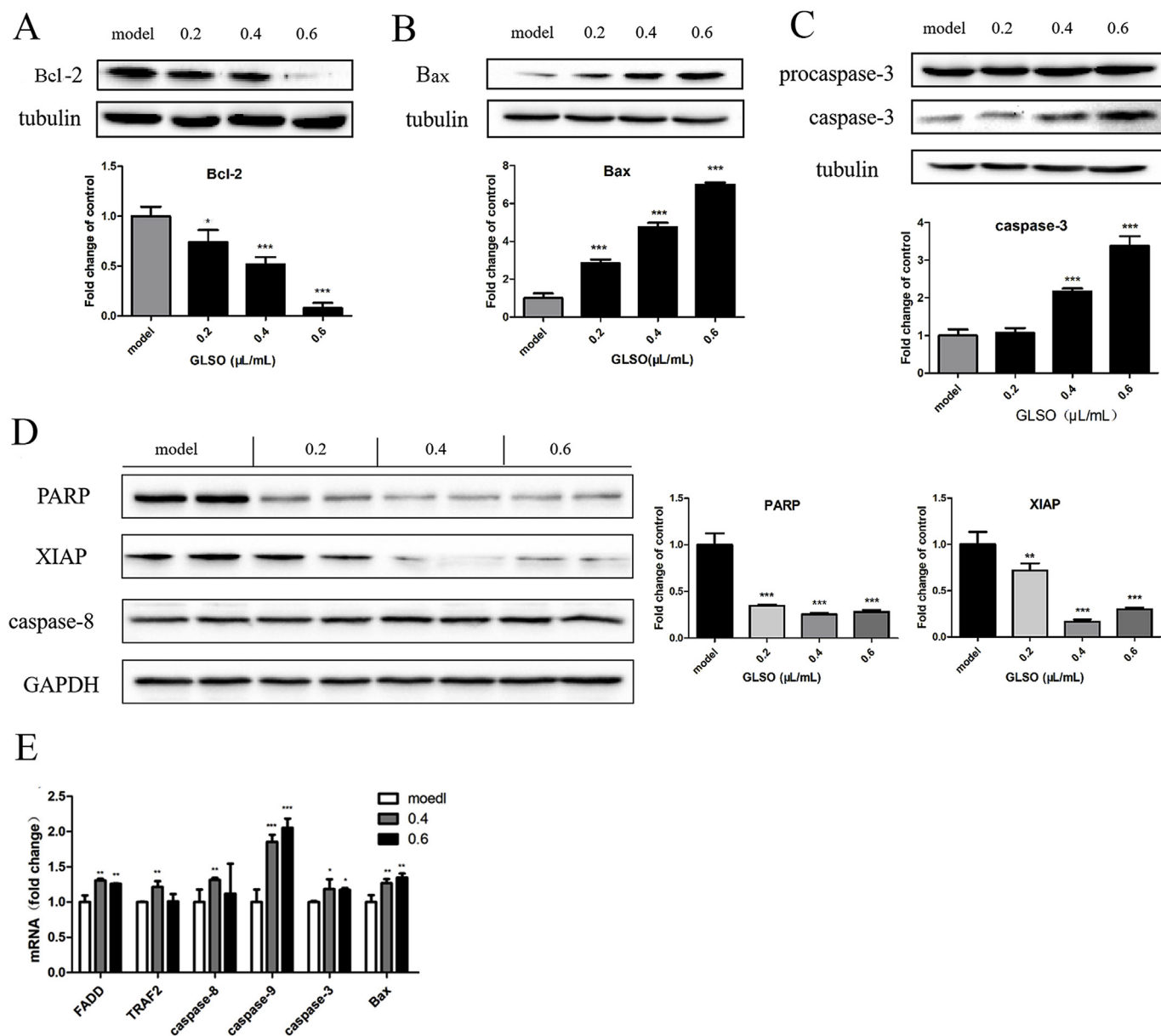
Fig. 2. Induction of apoptosis-related protein expression in MDA-MB-231 cells by GLSO. (A–D) Western blot analysis of the apoptosis-associated proteins Bcl-2, Bax, caspase-3, caspase-9, PARP and XIAP in MDA-MB-231 cells treated with the indicated concentrations of GLSO. Tubulin was analyzed as an internal control. Bands were quantified by densitometry and normalized to the model control values. (E) qRT-PCR analysis of mRNA levels of apoptosis-associated genes after treatment of MDA-MB-231 cells with the indicated concentrations of GLSO. β-Actin was analyzed as an internal control. mRNA levels were normalized to the model control values. Data are presented as the mean ± S.D. of three independent experiments. *$p < 0.05$, **$p < 0.01$, ***$p < 0.001$ vs model.

were observed in the GLSO-treated mice.

Next, the mechanism that GLSO inhibits tumor growth in vivo was studied by Western blot analysis of apoptosis-related proteins in excised tumor lysates. GLSO reduced the expression of total PARP, pro-caspase-9, and pro-caspase-3 in tumors compared with the model group. However, the expression of caspase-8 remained consistently (Fig. 3E), which was consistent with the in vitro findings with MDA-MB-231 cells. H&E staining of tumor sections revealed large necrotic areas in the tumors from the GLSO-treated mice compared with the model group. The necrotic areas were mainly characterized by the shallow staining area and pyknosis (Fig. 4A). To confirm the results of the Western blot analysis, we performed TUNEL staining to detect DNA double-strand breaks, which are characteristic of cells undergoing apoptosis. As expected, we found a significant increase in fluorescence labeling in tumor sections from the GLSO-treated group compared with the model group (Fig. 4B).

To examine the molecular mechanisms of inducing apoptosis by GLSO, immunohistochemical staining was used for tumor sections. The results showed that GLSO had upregulated the expression of the cytochrome c, caspase-9 and Bax, and downregulated the expression of the anti-apoptotic protein XIAP in tumors (Fig. 5).

3.4. GLSO induces apoptosis through the caspase pathway

Finally, in order to verify whether the apoptosis induced by GLSO involves the caspase pathway. MDA-MB-231 cells were pre-incubated with the caspase-3 (AZ10417808, ApexBio, A4416), caspase-8 (Z-IETD-FMK, ApexBio, B3232) and caspase-9 (Z-LEHD-FMK, ApexBio, B3233) inhibitors respectively for 3 h before the cells were incubated with GLSO for 16 h. The inhibition of GLSO on cell viability was significantly downregulated by AZ10417808 and Z-LEHD-FMK ($p < 0.01$), whereas Z-IETD-FMK had insignificant effect on cell viability (Fig. 6A). Western
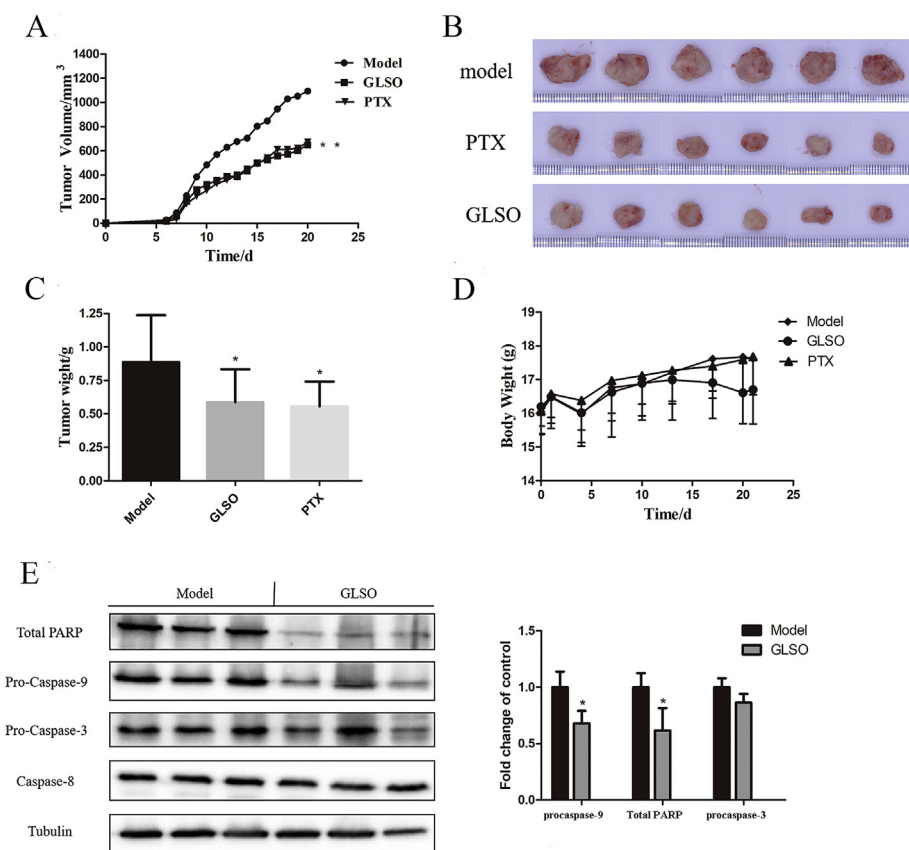
Fig. 3. GLSO inhibits the growth of 4T1 breast cancer cells in mice. (A–E) Mice were injected subcutaneously with 4T1 cells and left untreated (model) or treated with GLSO (6 g/kg/day) or paclitaxel (PTX, 10 mg/kg twice weekly) for 21 days, each with 12 animals/group. At the end of the experiment, mice were sacrificed and tumors were excised for analysis. (A) Tumor volumes. (B) Photograph of tumors excised at necropsy. (C) Average tumor weights at sacrifice. (D) Mouse body weights. (E) Western blot analysis of PARP and caspases-3, -8, and -9 in tumors excised at sacrifice. Tubulin was analyzed as an internal control. Bands were quantified by densitometry and normalized to the model control values. Data are presented as the mean ± S.D. of three independent experiments. *$p < 0.05$, **$p < 0.01$ vs model.

blot analysis showed that addition of the caspase inhibitors significantly increased the levels of pro-caspase-3, pro-caspase-9 and total PARP compared with GLSO alone, and also increased expression of the anti-apoptotic protein XIAP (Fig. 6B, C).

4. Discussion

In recent years, the natural product compounds have been widely concerned for prevention and treatment of cancer. Various classes of plant-derived anti-cancer agents, including polysaccharides, saponins, alkaloids, flavonoids and terpenoids, have been extensively studied at the preclinical and clinical levels. Cancer patients receiving conventional chemotherapy and radiotherapy often experience severe side effects, and TCMs are increasingly recognized as potentially less toxic adjunct or alternative cancer therapies (Parekh et al., 2009). *G. lucidum* is one of the most widely studied TCMs and has been used in East Asia for more than 2000 years to promote vitality and longevity. *G. lucidum* polysaccharides (GLP) extracted from *G. lucidum* has shown anti-cancer activity in several studies, and is thought to act *via* modulation of the immune system (Li et al., 2011; Xu et al., 2011), suppression of tumor angiogenesis (Cao and Lin, 2006), inhibition of cancer cell invasion and metastasis (Wu et al., 2006), inhibition of tumor cell proliferation, induction of tumor cell apoptosis (Sun et al., 2014), and suppression of drug resistance (Li et al., 2008). However, GLP contains peptidoglycans and glucose in addition to heteropolysaccharides and other polysaccharides (Bishop et al., 2015; Wasser, 2005). Due to its complexity and the limitations of separation and analytical techniques, the composition of GLP has not yet been fully identified. In addition to the spores, bioactive GLPs have been found in the fruiting bodies and mycelia of *G. lucidum*. (Ferreira et al., 2015). However, recent studies have found that BSGL not only contains more bioactive compounds than either the fruiting bodies or mycelia but also they have more potent anti-cancer activity than extracts of unbroken spores (Guo et al.,

2009; Huang et al., 2006; Zhao et al., 2006). Few studies have investigated the anti-tumor mechanisms of GLSO. For example, although Chen et al. (2016) examined the activity of *G. lucidum* extract and spore oil, they did not systematically study the mechanism of action.

Apoptosis is an ordered cell death process regulated by a complex and coordinated signaling network (Hanahan and Weinberg, 2000), and agents that can effectively induce apoptosis of cancer cells could have utility for therapy. In the present study, we found that GLSO induced apoptosis in MDA-MB-231 cells in a dose-dependent manner. Many studies have reported that Bcl-2 is highly expressed in cancer cells (Kobayashi et al., 2000; Paul-Samojedny et al., 2005), and overexpression of Bax increases apoptosis induced by chemotherapeutic agents (Kobayashi et al., 2000). Notably, the levels of caspase-3, caspase-9, and Bax mRNA were upregulated in GLSO-treated MDA-MB-231 cells, while Bcl-2 was downregulated. In addition, pro-caspase-9 and pro-caspase-3 protein levels were downregulated by GLSO, suggesting that it induces apoptosis *via* caspase activation. Indeed, it was confirmed that the anti-cancer activity of GLSO was significantly reduced by caspase inhibitors.

GLSO significantly inhibited the growth of 4T1 tumors in vivo. The results showed that GLSO had upregulated the expression of the cytochrome *c*, caspase-9 and Bax, and downregulated the expression of XIAP and total PARP in tumors. In addition, consistent with the results of this clinical trials, the results showed that GLSO had no obvious toxic effect on mice. For example, a prospective, randomized, double-blind, placebo-controlled study reported that intake of *G. lucidum* at 1.5 g/day for 4 weeks did not impair platelet or global hemostatic function and was demonstrated to be safe in healthy volunteers (Kwok et al., 2005). In another double-blind, placebo-controlled, randomized clinical study, Noguchi et al. (Noguchi et al., 2008) reported that *G. lucidum* ethanol extract administered at 6 mg daily was well tolerated and significantly improved lower urinary tract symptoms in men. Another controlled supplementation study in humans found that intake of *G. lucidum* for 4
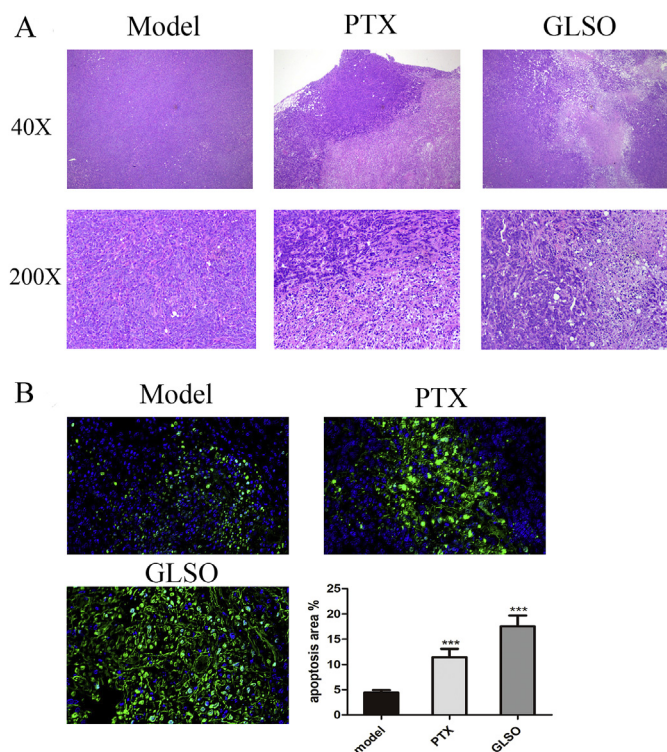
Fig. 4. GLSO induces apoptosis of 4T1 tumors in mice. (A and B) Mice were injected subcutaneously with 4T1 cells and treated as described for Fig. 2. Tumors were excised at sacrifice on day 21. (A) Images of H&E-stained tumor sections revealing areas of necrosis. (B) Fluorescence micrographs of TUNEL-stained tumor sections indicating apoptotic cells (green). Sections were also stained with DAPI (blue) to visualize nuclei. Magnification × 40 and × 200 (a) or × 400 (b).***$p < 0.001$ *vs* model. (For interpretation of the references to colour in this figure legend, the reader is referred to the Web version of this article.)

studies of the health benefits of GLSO compared with water or ethanol extracts in cancer patients. One randomized, double-blind, placebo-controlled study reported that a TCM herb complex containing whole extracts of *G. lucidum* significantly improved the immune function of cancer patients receiving chemotherapy and/or radiotherapy (Zhuang et al., 2009). However, more clinical trials will be needed to demonstrate GLSO as a new nutraceutical or drug for the prevention and treatment of breast cancer.

5. Conclusion

In conclusion, the present study demonstrated that GLSO inhibits the growth of MDA-MB-231 cells and tumors in vivo by inducing apoptosis, which may be achieved through the mitochondrial apoptotic pathway. Although further studies are needed to fully understand the mechanism of apoptosis induction, our results suggest that GLSO could be developed as a functional food or nutraceutical ingredient for chemotherapy.

Author contribution

Y.Z.X.* and B.B.Y.* conceived and designed the work; Y.Z.X.* and C.W.J. coordinated technical support and funding; C.W.J. and W.C. wrote the manuscript; X.P.T. and H.J.L. performed the experiments and collected the samples; Y.J.L. and H.Y.acquired, analyzed, and interpreted the data; C.Y.H., J.M.C and X.W.M. participated in data collection and analysis. All authors read and approved the final manuscript.

Declaration of competing interest

The authors declare no conflicts of interest.

Acknowledgments

weeks induced no toxicity (Wachtel-Galor et al., 2004). Although many preclinical studies have indicated the anti-cancer effects of *G. lucidum* triterpenoids, clinical studies are still lacking. Similarly, there are fewer
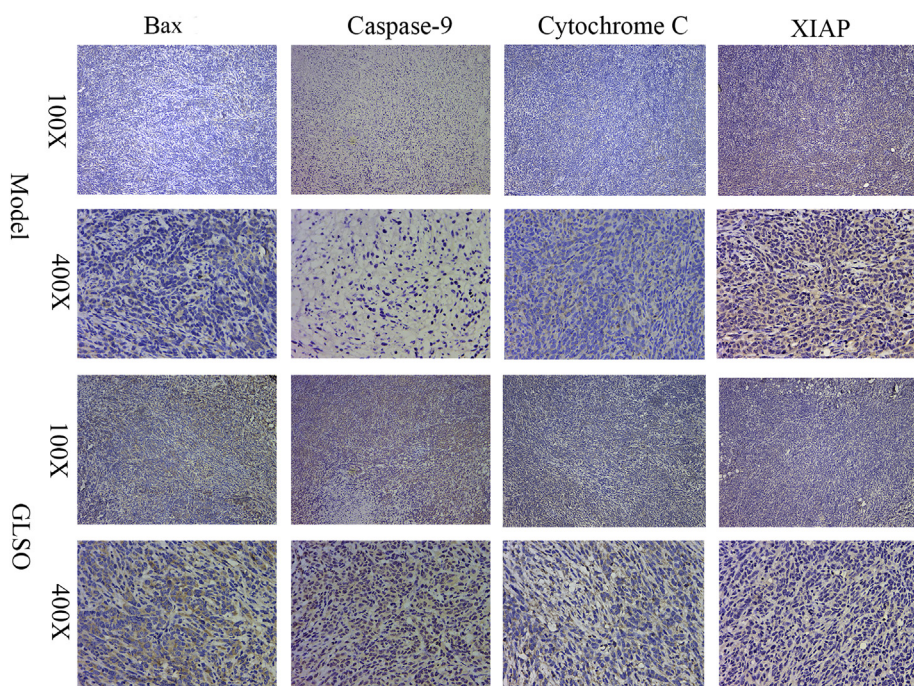

Fig. 5. GLSO inhibits cell proliferation and induces expression of apoptosis-related proteins in 4T1 tumors in mice. Mice were injected subcutaneously with 4T1 cells and treated as described for Fig. 2. Tumors were excised after sacrifice and subjected to immunohistochemical staining for caspase-9, Bax, XIAP, and cytochrome *c*. Magnification × 100 or × 400.
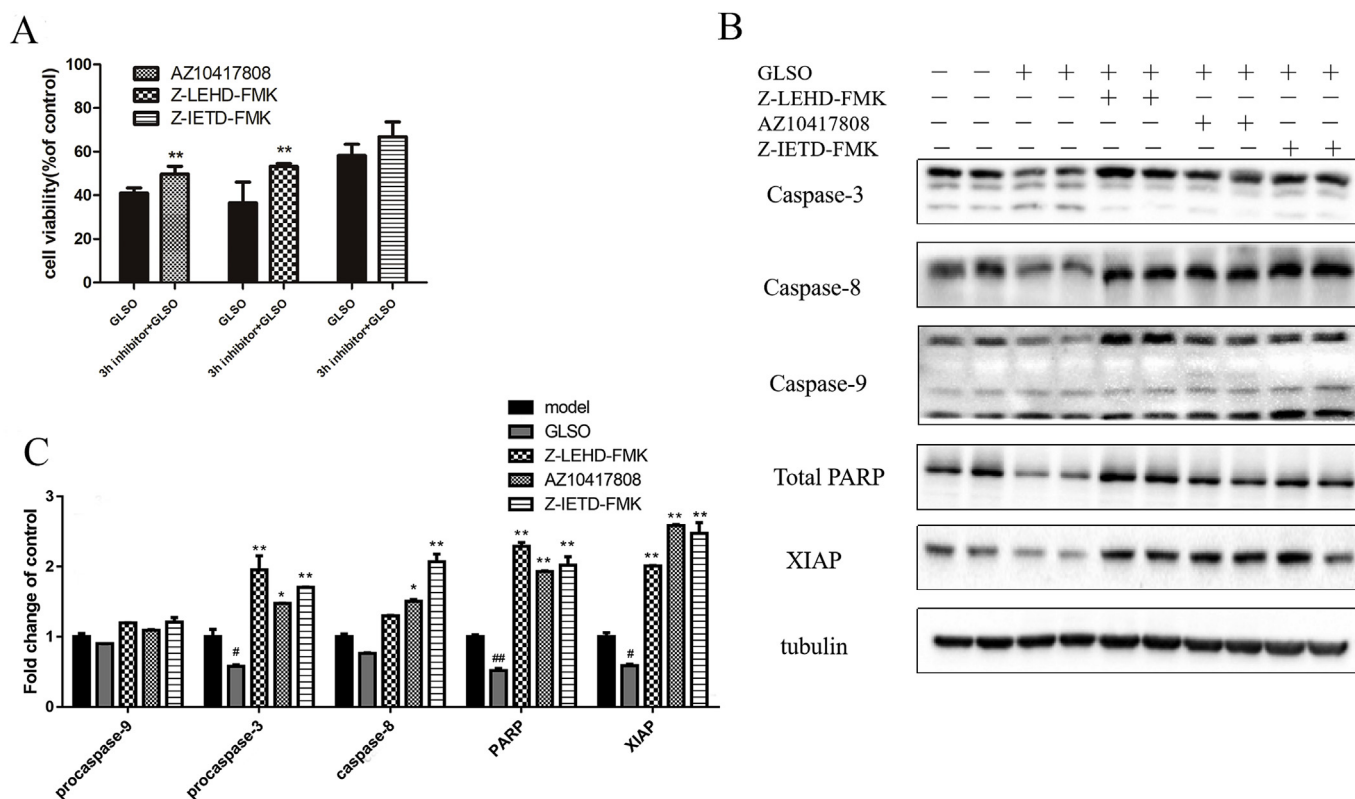
Fig. 6. Effect of caspase inhibitors on GLSO-induced apoptosis of MDA-MB-231 cells. (A) Viability of MDA-MB-231 cells pre-incubated for 3 h with AZ10417808 (caspase-3 inhibitor), Z-LEHD-FMK (caspase-9 inhibitor), or Z-IETD-FMK (caspase-8 inhibitor) prior to addition of GLSO for an additional 16 h. Viability was assessed by Trypan blue staining. (B–C) Western blot analysis of caspase-3, caspase-8, caspase-9, PARP and XIAP expression in MDA-MB-231 cells left untreated (model) or treated with GLSO or the indicated inhibitors with GLSO. Tubulin was analyzed as an internal control. (C) Densitometric quantification of the blot shown in (B). Bands were normalized to the model control values. Data are presented as the mean ± S.D. of three independent experiments. *$p < 0.05$, **$p < 0.01$ *vs* GLSO. [#]$p < 0.05$, [##]$p < 0.01$ *vs* model.

References

Akihisa, T., Nakamura, Y., Tagata, M., Tokuda, H., Yasukawa, K., Uchiyama, E., et al., 2007. Anti-inflammatory and anti-tumor-promoting effects of triterpene acids and sterols from the fungus *Ganoderma lucidum*. Chem. Biodivers. 4, 224–231.

Bao, P.P., Lu, W., Cui, Y., Zheng, Y., Gu, K., Chen, Z., Zheng, W., Shu, X.O., 2012. *Ginseng* and *Ganoderma lucidum* use after breast cancer diagnosis and quality of life: a report from the Shanghai Breast Cancer Survival Study. PLoS One 7 (6), e39343.

Barbieri, A., Quagliariello, V., Del Vecchio, V., Falco, M., Luciano, A., Amruthraj, N.J., Nasti, G., Ottaiano, A., Berretta, M., Iaffaioli, R.V., Arra, C., 2017. Anticancer and anti-inflammatory properties of *Ganoderma lucidum* extract effects on melanoma and triple-negative breast cancer treatment. Nutrients 9 (3), E210.

Bishop, K.S., Kao, C.H., Xu, Y., Glucina, M.P., Paterson, R.R., Ferguson, L.R., 2015. From 2000 years of *Ganoderma lucidum* to recent developments in nutraceuticals. Phytochemistry 114, 56–65.

Boh, B., Berovic, M., Zhang, J., Zhi-Bin, L., 2007. *Ganoderma lucidum* and its pharma-ceutically active compounds. Biotechnol. Annu. Rev. 13, 265–301.

Cao, Q.Z., Lin, Z.-B., 2006. *Ganoderma lucidum* polysaccharides peptide inhibits the growth of vascular endothelial cell and the induction of VEGF in human lung cancer cell. Life Sci. 78, 1457–1463.

Chawla-Sarkar, M., Leaman, D.W., Borden, E.C., 2001. Preferential induction of apoptosis by interferon (IFN)-beta compared with IFN-alpha2: correlation with TRAIL/Apo2L induction in melanoma cell lines. Clin. Cancer Res. 7 (6), 1821–1831.

Chen, C., Li, P., Li, Y., Yao, G., Xu, J.H., 2016. Antitumor effects and mechanisms of *Ganoderma* extracts and spores oil. Oncol Lett 12 (5), 3571–3578.

Dan, X., Liu, W., Wong, J.H., Ng, T.B., 2016. A ribonuclease isolated from wild *Ganoderma lucidum* suppressed autophagy and triggered apoptosis in colorectal cancer cells. Front. Pharmacol. 7, 217.

el-Mekkawy, S., Meselhy, M.R., Nakamura, N., Tezuka, Y., Hattori, M., Kakiuchi, N., Shimotohno, K., Kawahata, T., Otake, T., 1998. Anti-HIV-1 and anti-HIV-1-protease substances from *Ganoderma lucidum*. Phytochemistry 49, 1651–1657.

Ferlay, J., Colombet, M., Soerjomataram, I., 2019. Estimating the global cancer incidence and mortality in 2018: GLOBOCAN sources and methods. Int. J. Cancer 144 (8), 1941–1953.

Ferreira, I.C., Heleno, S.A., Reis, F.S., Stojkovic, D., Queiroz, M.J., Vasconcelos, M.H., Sokovic, M., 2015. Chemical features of *Ganoderma* polysaccharides with antioxidant, antitumor and antimicrobial activities. Phytochemistry 114, 38–55.

Guo, L., Xie, J., Ruan, Y., Zhou, L., Zhu, H., Yun, X., Jiang, Y., Lü, L., Chen, K., Min, Z.,

Wen, Y., Gu, J., 2009. Characterization and immunostimulatory activity of a poly-saccharide from the spores of *Ganoderma lucidum*. Int. Immunopharmacol. 9, 1175–1182.

Hanahan, D., Weinberg, R.A., 2000. The hallmarks of cancer. Cell 100, 57–70.

Hu, H., Ahn, N.S., Yang, X., Lee, Y.S., Kang, S., 2002. *Ganoderma lucidum* extract induces cell cycle arrest and apoptosis in MCF-7 human breast cancer cell. Int. J. Cancer 102, 250–253.

Huang, X.L., Hui-Qin, W.U., Fang, H., Lin, X.S., 2006. Analysis of polysaccharide from broken cellular wall and unbroken spore of *Ganoderma lucidum*. Chin. Tradit. Herb. Drugs 37, 813–816.

Huie, C.W., Di, X., 2004. Chromatographic and electrophoretic methods for Lingzhi pharmacologically active components. J. Chromatogr. B 812, 241–257.

Jang, S.H., Cho, S.W., Yoon, H.M., Jang, K.J., Song, C.H., Kim, C.H., 2014. Hepatoprotective evaluation of *Ganoderma lucidum* pharmaco-puncture: in vivo stu-dies of ethanol-induced acute liver injury. J. Pharmacopuncture 17, 16–24.

Jiao, C.W., Liang, H.J., Jian, W.M., 2014. Effects of *Ganoderma lucidum* spore oil on caspase-3 activity and the apoptotic process in MT-1 human breast cancer cells. Acta Edulis Fungi 21 (04), 58–60.

Jin, X., Ruiz Beguerie, J., Sze, D.M.Y., Chan, G.C.F., 2016. *Ganoderma lucidum* (Reishi mushroom) for cancer treatment (review). Cochrane Database Syst. Rev. 4, 1–37.

Ko, H.H., Hung, C.F., Wang, J.P., Lin, C.N., 2008. Antiinflammatory trit-erpenoids and steroids from *Ganoderma lucidum* and *G. tsugae*. Phytochemistry 69, 234–239.

Kobayashi, T., Sawa, H., Morikawa, J., Zhang, W., Shiku, H., 2000. Bax induction acti-vates apoptotic cascade via mitochondrial cyto-chrome c release and Bax over-expression enhances apoptosis induced by chemotherapeutic agents in DLD-1 colon cancer cells. Jpn. J. Cancer Res. 91, 1264–1268.

Koyama, K., Imaizumi, T., Akiba, M., Kinoshita, K., Takahashi, K., Suzuki, A., Yano, S., Horie, S., Watanabe, K., Naoi, Y., 1997. Anti-nociceptive components of *Ganoderma lucidum*. Planta Med. 63, 224–227.

Kwok, Y., Ng, K.F., Li, C.C., Lam, C.C., Man, R.Y., 2005. A prospective, randomized, double-blind, placebo-controlled study of the platelet and global hemostatic effects of *Ganoderma lucidum* (Ling-Zhi) in healthy volunteers. Anesth. Analg. 101, 423–426.

Lam, F.F., Ko, I.W., Ng, E.S., Tam, L.S., Leung, P.C., Li, E.K., 2008. Analgesic and anti-arthritic effects of Lingzhi and San Miao San supplementation in a rat model of ar-thritis induced by Freund's complete adjuvant. J. Ethnopharmacol. 120, 44–50.

Li, W.D., Zhang, B.D., Wei, R., Liu, J.H., Lin, Z.B., 2008. Reversal effect of *Ganoderma lucidum* polysaccharide on multidrug resistance in K562/ADM cell line. Acta Pharmacol. Sin. 29, 620–627.

Li, W.J., Chen, Y., Nie, S.P., Xie, M.Y., He, M., Zhang, S.S., Zhu, K.X., 2011. *Ganoderma*

atrum polysaccharide induces anti-tumor activity via the mitochondrial apoptotic pathway related to activation of host immune response. J. Cell. Biochem. 112, 860–871.

Min, B.S., Nakamura, N., Miyashiro, H., Bae, K.W., Hattori, M., 1998. Triterpenes from the spores of *Ganoderma lucidum* and their inhibitory activity against HIV-1 protease. Chem. Pharm. Bull. (Tokyo) 46, 1607–1612.

Mowsumi, F.R., Rahman, M.M., Rahaman, A., Selina, F.A., Islam, M.J., Bhuiyan, M.H.S., 2013. Preventive effect of *Ganoderma lucidum* on paraetamol-induced acute hepato-toxicity in rats. Bangladesh J. Sci. Res. 5, 573–578.

Naito, S., von Eschenbach, A.C., Giavazzi, R., Fidler, I.J., 1986. Growth and metastasis of tumor cells isolated from a human renal cell carcinoma implanted into different organs of nude mice. Cancer Res. 46 (8), 4109–4115.

Noguchi, M., Kakuma, T., Tomiyasu, K., Yamada, A., Itoh, K., Konishi, F., Kumamoto, S., Shimizu, K., Kondo, R., Matsuoka, K., 2008. Randomized clinical trial of an ethanol extract of *Ganoderma lucidum* in men with lower urinary tract symptoms. Asian J. Androl. 10, 777–785.

Parekh, H.S., Liu, G., Wei, M.Q., 2009. A new dawn for the use of traditional Chinese medicine in cancer therapy. Mol. Cancer 8, 21.

Paul-Samojedny, M.1., Kokocińska, D., Samojedny, A., Mazurek, U., Partyka, R., Lorenz, Z., Wilczok, T., 2005. Expression of cell survival/death genes: Bcl-2 and Bax at the rate of colon cancer prognosis. Biochim. Biophys. Acta 1741 (1–2), 25–29.

Sun, Z., Huang, K., Fu, X., Zhou, Z., Cui, Y., Li, H., 2014. A chemically sulfated poly-saccharide derived from *Ganoderma luciduminduces* mitochondrial-mediated apoptosis in human osteo- sarcoma MG63 cells. Tumour Biol 35, 9919–9926.

Wachtel-Galor, S., Szeto, Y.T., Tomlinson, B., Benzie, I.F., 2004. *Ganoderma lucidum* ('Lingzhi'); acute and short-term biomarker response to supplementation. Int. J. Food Sci. Nutr. 55, 75–83.

Wasser, S.P., 2005. Reishi or ling zhi (*Ganoderma lucidum*). In: Blackman, M.R., Cragg, G.M., Levine, M., Moss, J., White, J.D. (Eds.), Encyclopedia of Dietary Supplements.Coates PM. Marcel Dekker, New York, pp. 603–622.

Wu, Q.P., Xie, Y.Z., Li, S.Z., La Pierre, D.P., Deng, Z., Chen, Q., Zhang, Z., Guo, J., Wong, A.C., Lee, D.Y., Yee, A., Yang, B.B., 2006. Tumour cell adhesion and integrin expression affected by *Ganoderma lucidum*. Enzym. Microb. Technol. 40, 32–41.

Wu, G., Qian, Z., Guo, J., Hu, D., Bao, J., Xie, J., Xu, W., Lu, J., Chen, X., Wang, Y., 2012. *Ganoderma lucidum* extract induces G1 cell cycle arrest, and apoptosis in human breast cancer cells. Am. J. Chin. Med. 40, 631–642.

Wu, G.S., Guo, J.J., Bao, J.L., Li, X.W., Chen, X.P., Lu, J.J., Wang, Y.T., 2013. Anti-cancer properties of triterpenoids isolated from *Ganoderma lucidum*-a review. Expert Opin. Investig. Drugs 22, 981–992.

Xu, Z., Chen, X., Zhong, Z., Chen, L., Wang, Y., 2011. *Ganoderma lucidum* polysaccharides: immunomodulation and potential antitumor activities. Am. J. Chin. Med. 39, 15–27.

Zhao, J., Qiu, C., Li, J., Fan, J., Chen, K., 2006. Inhibitive effect of seleniumenriching wall-broken *Ganoderma lucidum* spore powder on HepG2 cells. Life Sci. 79, 1129.

Zhao, H., Zhang, Q., Zhao, L., Huang, X., Wang, J., Kang, X., 2012. Spore Powder of Ganoderma Lucidum Improves Cancer-Related Fatigue in Breast Cancer Patients Undergoing Endocrine Therapy: A Pilot Clinical Trial. Evid Based Complement Alternat Med. pp. 809614.

Zhuang, S.R., Chen, S.L., Tsai, J.H., Huang, C.C., Wu, T.C., Liu, W.S., Tseng, H.C., Lee, H.S., Huang, M.C., Shane, G.T., Yang, C.H., Shen, Y.C., Yan, Y.Y., Wang, C.K., 2009. Effect of citronellol and the Chinese medical herb complex on cellular immunity of cancer patients receiving chemotherapy/radio-therapy. Phytother Res. 23, 785–790.